HHS Public Access

Author manuscript

J Comp Neurol. Author manuscript; available in PMC 2016 March 21.

Published in final edited form as:

J Comp Neurol. 2013 October 15; 521(15): 3508–3523. doi:10.1002/cne.23367.

Hilar Interneuron Vulnerability Distinguishes Aged Rats With Memory Impairment

Amy M. Spiegel[1], **Ming Teng Koh**[1], **Nicholas M. Vogt**[2], **Peter R. Rapp**[3], and **Michela Gallagher**[1,*]

[1]Department of Psychological and Brain Sciences, Johns Hopkins University, Baltimore, Maryland 21218

[2]Department of Psychology, Swarthmore College, Swarthmore, Pennsylvania 19081

[3]Laboratory of Behavioral Neuroscience, National Institute on Aging, Baltimore, Maryland 21224

Abstract

Hippocampal interneuron populations are reportedly vulnerable to normal aging. The relationship between interneuron network integrity and age-related memory impairment, however, has not been tested directly. That question was addressed in the present study using a well-characterized model in which outbred, aged, male Long-Evans rats exhibit a spectrum of individual differences in hippocampal-dependent memory. Selected interneuron populations in the hippocampus were visualized for stereological quantification with a panel of immunocytochemical markers, including glutamic acid decarboxylase-67 (GAD67), somatostatin, and neuropeptide Y. The overall pattern of results was that, although the numbers of GAD67- and somatostatin-positive interneurons declined with age across multiple fields of the hippocampus, alterations specifically related to the cognitive outcome of aging were observed exclusively in the hilus of the dentate gyrus. Because the total number of NeuN-immunoreactive hilar neurons was unaffected, the decline observed with other markers likely reflects a loss of target protein rather than neuron death. In support of that interpretation, treatment with the atypical antiepileptic levetiracetam at a low dose shown previously to improve behavioral performance fully restored hilar SOM expression in aged, memory-impaired rats. Age-related decreases in GAD67- and somatostatin-immunoreactive neuron number beyond the hilus were regionally selective and spared the CA1 field of the hippocampus entirely. Together these findings confirm the vulnerability of hippocampal interneurons to normal aging and highlight that the integrity of a specific subpopulation in the hilus is coupled with age-related memory impairment.

*CORRESPONDENCE TO: Michela Gallagher, PhD, Department of Psychological and Brain Sciences, Johns Hopkins University, 3400 N. Charles St., Baltimore, MD 21218. michela@jhu.edu.

CONFLICT OF INTEREST STATEMENT

MG and MTK are inventors on Johns Hopkins University intellectual property licensed to AgeneBio. MG has a financial interest in the company. MTK has received no financial support or compensation from any individual or corporate entity for research or professional services and has no financial holdings that could be perceived as constituting a potential conflict of interest.

ROLE OF AUTHORS

All authors had full access to all the data in the study and take responsibility for the integrity of the data and the accuracy of the data analysis. Study concept and design: AMS, MG. Acquisition of data: AMS, MTK, NMV. Analysis and interpretation of data: AMS, PRR, MG. Drafting and revision of the manuscript: AMS, PRR, MG.

INDEXING TERMS

hippocampus; interneuron; somatostatin; neuropeptide Y; stereology; levetiracetam

Memory loss is one of the most prevalent concerns in the aging population and is attributed to changes in the functional properties of hippocampal circuits. Recent evidence indicates that a failure to maintain a proper balance of excitatory and inhibitory control affects specific components of the hippocampal network when memory loss occurs (Wilson et al., 2005a; Yassa et al., 2011). Studies examining individuals with age-related memory loss or amnestic mild cognitive impairment (aMCI, i.e., deficits greater than would be expected for a person's age) have shown increased activation in the hippocampus localized to the dentate gyrus (DG)/CA3 subregion on high-resolution functional magnetic resonance imaging (fMRI; Yassa et al., 2010, 2011). Similar patterns of aberrant hippocampal activity occur in aged, memory-impaired rats, in which increased CA3 neuronal activity correlates with impaired pattern separation function and the inability to rapidly encode new information (Wilson et al., 2005a). Together these data suggest that a decline in inhibitory control within the aged hippocampus might contribute to excess activation affecting specific subregions of the hippocampal network.

Inhibitory input from γ-aminobutyric acid (GABA)-ergic interneurons regulates pyramidal and granule cell excitability in the hippocampus, setting the threshold required for excitation and coordinating discharge activity. In the DG and CA3 subregions, interneurons contribute to sparse hippocampal encoding by precisely timing granule cell firing and restricting the powerful CA3-recurrent collateral network (Freund and Buzsaki, 1996; Houser, 2007; Myers and Scharfman, 2009). Ablation of hippocampal interneurons is known to produce conditions of excess excitation in this network, and models of epilepsy have suggested that a functional failure or degeneration of hippocampal interneurons contributes the aberrant excitatory activity that characterizes that disease (Halabisky et al., 2010; Ratzliff et al., 2004; Sun et al., 2007; Vezzani et al., 1996). Given the role of GABAergic interneurons in regulating hippocampal excitability, it seems plausible that age-related alterations to hippocampal interneuron networks might also contribute to the excess activity observed in the aged hippocampus contributing to the associated memory impairment.

Previous research provides evidence that a decline in hippocampal interneuron integrity is associated with normal brain aging (Gavilan et al., 2007; Hattiangady et al., 2005; Shetty and Turner, 1998; Shi et al., 2004; Stanley and Shetty, 2004; Stanley et al., 2012). However, prior investigations have not typically identified the cognitive status of aged subjects to determine the relationship between hippocampal interneuron integrity and cognitive decline. To examine whether changes in hippocampal interneuron integrity are associated with age-related memory loss, the present study used unbiased, design-based stereology to determine the total number of glutamic acid decarboxylase-67 (GAD67)-immunopositive interneurons throughout all subregions of the hippocampus in young, aged memory-unimpaired, and aged memory-impaired Long-Evans rats (Gallagher et al., 1993). In this model, aged rats exhibit stable individual differences in cognitive status during aging as determined by hippocampal-dependent behavioral assessments. An antibody against GAD67, the constituently active

isoform of the GABA-synthesizing enzyme, was used to visualize GABAergic interneuron cell bodies (Freund and Buzsaki, 1996; Shetty and Turner, 1998; Shi et al., 2004; Stanley and Shetty, 2004). Decreased numbers of GAD67-expressing interneurons were observed in the hilus of the DG in aged rats with memory impairment, so total hilar neuron number was quantified to determine whether the decrease in GAD67-immunoreactive interneuron numbers was associated with neuronal loss, which has previously been reported in the dentate hilus of older adults (West, 1993). This analysis involved stereological estimation of the number of hilar neurons expressing neuronal nuclei protein (NeuN), a neurochemical marker expressed by all interneurons. In addition, to understand better which subtypes of hilar inhibitory interneurons are most susceptible to the effects of aging, the numbers of somatostatin (SOM)- and neuropeptide Y (NPY)-immunoreactive hilar neurons were stereologically quantified in tissue from the same young, aged memory-unimpaired, and aged memory-impaired Long-Evans rats utilized in the GAD67 and NeuN analyses. Based on the outcome of those experiments, a final, targeted analysis in separate groups of young and aged rats tested whether SOM-positive interneurons in the hilus are sensitive to a pharmacological intervention known to benefit memory in aged impaired rats (Koh et al., 2010).

MATERIALS AND METHODS

Animals

All animal procedures followed NIH guidelines and were approved by the Animal Care and Use Committee of Johns Hopkins University. Aged, male Long-Evans rats were obtained at 8–9 months of age from Charles River Laboratories (Raleigh, NC) and housed in a vivarium at Johns Hopkins University until 24–26 months of age. Young male rats obtained from the same source were housed in the same vivarium and tested at 6 months of age. All rats were individually housed and maintained on a 12-hour light/dark cycle. Food and water were provided ad libitum, and rats were determined to be healthy and free of pathogenesis and disability.

Behavioral characterization

Rats were behaviorally characterized for spatial memory using water maze task procedures previously described in detail (Gallagher et al., 1993; Haberman et al., 2011). Behavioral testing took place during the light phase, over 8 training days in sessions of three trials per day. At the start of each trial, rats were placed in the water at the perimeter of the pool, with starting locations varied across trials. Individual trials lasted for 90 seconds or until the rat successfully located the platform, with a 60-second intertrial interval. Every sixth trial was a probe trial to assess the rat’s spatial bias during its search. After 30 seconds during probe trials, a platform was raised and rats were permitted to escape. The primary measure used to assess performance in the spatial learning task was proximity to the escape platform, one of the more sensitive measures of behavioral performance in this task (Maei et al., 2009). A memory index score, derived from the proximity of the rat to the platform location during the 30-second free swim on probe trials, was used to characterize performance in the maze. This index is the sum of the weighted proximity scores measured during probe trials, with lower scores reflecting more accurate searching close to the platform location (Gallagher et

al., 1993). Aged rats that performed within the normative range of the young were characterized as aged memory-unimpaired, and those performing worse were classified as aged memory-impaired. Cue training (visible platform) was conducted on the last day of training to test for sensorimotor and motivational factors that could influence task performance independent of spatial learning and memory, and rats with cue training deficits were excluded from further study.

Perfusion and tissue preparation

Approximately 1 month after behavioral characterization, rats were anesthetized with isoflurane and perfused transcardially with sterile saline, followed by 4% paraformaldehyde in phosphate buffer (pH 7.2). After 24 hours of postfixation at 4°C, brains were moved into 30% sucrose (16% sucrose for levetiracetam-treated and vehicle-injected control animals; see description below) in phosphate buffer for 24 hours at 4°C. Whole brains were immediately frozen on powdered dry ice and stored at −80°C until histological processing. Tissue was sectioned in the coronal plane at a nominal 40 μm thickness on a freezing microtome. Sections were stored in cryoprotectant (25% ethylene glycol, 25% glycerol, 50% 0.1 M phosphate buffer, pH 7.2) at −20°C.

Antibody characterization

Mouse anti-GAD67—The anti-GAD67 antiserum was raised against a recombinant fusion protein containing the N-terminal regions (amino acids 4–101) of human GAD67 (Chemicon, Billerica, MA; catalog No. MAB5406) and shows no cross-reactivity with the 65-kDa isoform of GAD in rat brain lysates (manufacturer's technical information). This antibody against GAD67 has published specificity (Fong et al., 2005) and Western blot analysis of rat hippocampal protein extracts performed for the current study and a previous study revealed a single band at 67 kDa (Stranahan et al., 2012). As expected, the staining showed dense labeling localized to the neuronal cytoplasm and proximal axons and dendrites. Expected staining patterns were based on comparisons with previously published reports using anti-GAD67 antiserum (Fetissov et al., 2009; Shetty and Turner, 1998; Shi et al., 2004; Singec et al., 2004; Stanley and Shetty, 2004).

Mouse anti-NeuN—The anti-NeuN antiserum, raised against cell nuclei purified from mouse brain, recognizes two or three bands in the 46–48-kDa range and another band at ~66 kDa on Western blot (manufacturer's technical information) and has published specificity (Chemicon; catalog No. MAB377; Mullen et al., 1992). Consistent with previous reports, staining for the NeuN antiserum was observed in neuronal cell bodies exclusively (Mullen et al., 1992; Stanley and Shetty, 2004).

Rabbit anti-NPY—The anti-NPY antiserum was raised in rabbit against synthetic porcine NPY conjugated to keyhole limpet hemocyanin (KLH); recognizes human, rat, porcine, and sheep NPY; and cross-reacts with human peptide YY. The anti-NPY antiserum does not cross-react with neurokinin B, neurokinin A, substance P, calcitonin, or SOM (manufacturer's certificate of analysis). We validated the anti-NPY antiserum in the current study by preincubation with the immunizing peptide (Sigma-Aldrich, St. Louis, MO; catalog No. N5017), which eliminated immunostaining in rat brain, consistent with previous

observations (Real et al., 2009; Ruscheweyh et al., 2007). Immunoreactivity showed the expected pattern of dense cytoplasmic signal, with partial labeling of axons and dendrites. The expected labeling pattern was derived from previous descriptions in studies using a different antibody against NPY (Sun et al., 2007; Vezzani et al., 1996). The distribution of NPY-immunoreactive cells was similar to that observed via in situ hybridization for NPY mRNA (Vezzani et al., 1996).

Goat anti-SOM—The anti-SOM antiserum used here was raised in goat against synthetic peptide LELQRSANSNPAMAPRERK, corresponding to amino acids 84–102 of human SOM, and recognizes a single band at ~14 kDa on Western blot (manufacturer's technical information). Specificity was validated in the current work by preincubation with the immunizing peptide (Santa Cruz Biotechnology, Santa Cruz, CA; catalog No. SC7819-P), confirming published findings using Western blotting (Santa Cruz Biotechnology; catalog No. SC7819; Real et al., 2009). The anti-SOM antiserum showed the expected pattern of labeling, with dense cytoplasmic signal and relatively extensive axonal and dendritic labeling. The anticipated staining pattern was based on earlier descriptions of labeling in the rat DG seen with other antibodies against SOM (Sun et al., 2007; Vezzani et al., 1996). The distribution of SOM-immunoreactive cells observed here was also similar to that revealed by in situ hybridization for SOM mRNA (Vezzani et al., 1996).

Immunohistochemistry

The present study used immunocytochemical labeling and quantification of immunoreactive cell number as a probe for the overall network integrity of defined interneuron populations in the aged hippocampus. For each antibody, a single series was labeled using an established immunoperoxidase protocol, and histological sections from all conditions were processed concurrently to minimize interreplication variability (Haberman et al., 2011). Briefly, free-floating sections were washed in 0.1 M phosphate-buffered saline (PBS) to remove cryoprotectant, and endogenous peroxidases were quenched in 0.3% H_2O_2 in PBS. After additional PBS washes, sections were blocked in 5% normal horse serum in PBS with 0.3% Triton. Sections were then incubated with primary antibody at the predetermined optimal dilution (Table 1) in PBS containing 0.15% Triton and 3% normal serum for 72 hours (48 hours for NeuN) at 4°C with agitation. Material from levetiracetam-treated and associated vehicle control rats (described below) was processed separately according to a slightly modified protocol for SOM immunolabeling (primary antibody dilution 1:1,600). After primary antibody incubation, sections were washed in PBS and reacted with biotinylated secondary antibody goat anti-mouse or anti-rabbit or horse anti-goat IgG (Vector, Burlingame, CA) diluted in PBS with 0.15% Triton and 5% normal horse serum for 45 minutes. The secondary antibody was detected with avidin-biotin complex (ABC Elite; Vector), and the avidin-biotin complex was visualized with nickel-enhanced diaminobenzidine (Vector). Tissue sections were mounted onto gelatin-coated slides and dried, dehydrated with increasing ethanol concentrations, cleared in xylene, and coverslipped using DPX mounting media.

Unbiased stereology

Interneuron quantification was performed using a Zeiss Axioplan 2 microscope equipped with a motorized stage under the control of MBF Stereo Investigator software (version 9.10.4; Bioscience MicroBrightField, Williston, VT). The optical fractionator method was applied, which is an efficient, unbiased stereological probe for counting objects within thick tissue sections (Rapp and Gallagher, 1996; West et al., 1991). All analyses were conducted blind with regard to animal age and cognitive status. Interneurons were quantified throughout the rostrocaudal extent of each hippocampal subregion and lamina, including the CA1 and CA3 stratum oriens, pyramidal, radiatum, lacunosum-moleculare; and DG stratum granulosum, stratum moleculare, and polymorphic or hilar region of the DG. Neuron counts were derived from a minimum of 10 histological sections, spaced at 400 μm throughout the entire rostrocaudal extent of the dorsal and ventral hippocampus. Counts were derived unilaterally and estimates multiplied by 2 for the GAD67 and NeuN analyses in instances in which unilateral hippocampal tissue damage occurred during processing. Differences in comparison with neuron number estimated from bilateral counts were negligible. Regions of interest were defined according to the Paxinos and Watson rat brain atlas (1997) and digitized under a ×5 objective lens. Counts were taken with a ×100/1.4 numerical aperture oil-immersion objective in every subfield and sublayer and surveyed at evenly spaced X–Y intervals no greater than 150 μm × 150 μm. Figure 1 depicts GAD67-, SOM-, NPY-, and NeuN-immunoreactive hilar neurons at a magnification similar to that used for quantification. The dimensions of the unbiased counting frame were set to 50 μm × 50 μm for neuropeptide-containing cells and to 25 μm × 25 μm in the case of NeuN. Counting was further confined to no greater than 14 μm centered within the thickness, or z-axis, of the histological sections, and guard zones of 3 μm were used to eliminate potential biases introduced by the cutting process (appropriate sampling parameters were derived from preliminary test-tissue analysis). Section thickness was recorded at each site. The sampling scheme was established to obtain individual estimates of neuron number in each hippocampal subregion with estimated coefficients of error (CE) of about 0.10. The specific stereological sampling parameters utilized for each marker and anatomical region are given in Table 2. StereoInvestigator software was used to calculate total neuron number and the corresponding coefficient of error. Because the GAD67, NPY, and SOM stains obscured the nucleus, the most superficial point at which the cell soma was visibly filled with the diaminobenzidine reaction product was identified and used as the counting unit. For NeuN staining, neurons were counted if the top of the nucleus first came into focus within the boundaries of the optical dissector. Digital photomicrographs were acquired in StereoInvestigator and adjusted for brightness and contrast in Adobe Photoshop (Adobe Systems, San Jose, CA).

Based on the outcome of the GAD67 and SOM analyses, a targeted followup in separate groups of young and aged memory-impaired (AI) rats tested the possibility that levetiracetam, administered at a dose known to improve memory in aged impaired rats, also rescues SOM expression in the hilus. For this purpose, four anatomically matched (bregma −3.80 mm to −4.16 mm), immunolabeled sections each from young (n = 6), levetiracetam-treated AI (n = 6), and saline vehicle-treated AI (n = 6) were prepared, and the number of SOM-positive neurons in the hilus was counted exhaustively, under a ×40 objective. All

sections were processed together, and the counting was performed blind with respect to the age and treatment condition of the subjects.

Surgery and levetiracetam treatment

To test the effect of levetiracetam on SOM expression in hilar interneurons in aged rats with memory deficits, six young adults and 12 aged impaired rats were studied after behavioral characterization using the standard protocol. Under isoflurane anesthesia, the memory-impaired aged rats were implanted subcutaneously in the intrascapular region with osmotic minipumps (Alzet; Durect Corporation, Cupertino, CA) with levetiracetam (10 mg/kg/day; n = 6) or saline vehicle (n = 6) for 4 weeks prior to perfusion. The aged rats assigned to these treatment conditions had comparable severity of memory impairment prior to treatment (AI-VEH, memory index score = 286, SEM ± 10.8; AI-LEV, memory index score = 282, SEM ± 19.8; $t_{10} = 0.170$, $P = 0.869$). The behavioral benefit of levetiracetam administration on age-related memory impairment in this model has been reported elsewhere (Koh et al., 2010). Young rats, which served as controls, received either saline vehicle in minipumps or no implantation. At the end of the 4-week treatment, rats were euthanized and the brains processed as described above.

Statistical analysis

Total cell counts for each immunocytochemical marker were compared across young, AU, and AI rats for each hippocampal field and sublayer using one-way ANOVA (SPSS 19.0.0 for Mac OS X). Because changes in neuron numbers were proportional along the dorsoventral axis, the data were collapsed across sections through the dorsal and ventral hippocampus. Scheffe's post hoc analyses were conducted when the overall group ANOVA reached significance. This conservative post hoc test protects against type 1 errors and is appropriate in cases with unequal sample sizes, such as the current study. Pearson's *r*, two-tailed correlations between interneuron number in each hippocampal sublayer/subregion, and memory index score were computed to determine whether interneuron counts were coupled with cognitive status among animals in the aged cohort, i.e., with young rats excluded (for methodological issues see Baxter and Gallagher, 1996).

RESULTS

Behavioral assessment of cognitive status

Hippocampal-dependent memory was assessed with a protocol extensively used in this study population to detect cognitive status in healthy, aged rats. Performance during training trials with the hidden platform revealed proficient acquisition and retention of spatial memory in young adult rats (Fig. 2A). Search error, reflecting deviations from a direct path to the platform, declined over the course of training, with young rats achieving optimal performance by the fourth block of training trials. Aged rats did not differ from young in their performance on the first trial but were significantly less proficient in the task over the course of training (repeated-measures ANOVA for search error, $F_{1,21} = 11.01$, $P = 0.003$; Fig. 2A). Performance during probe trials, used to determine search accuracy, provided index scores for young rats, which were in the normative range for this study population, with lower values indicating search in closer proximity to the target location (Fig. 2B). As

expected, the aged rats exhibited higher index scores than young overall (young mean [SEM] = 203.56 [9.86], aged mean [SEM] = 242.58 [12.95], $F_{2,20} = 35.496$, $P < 0.001$) but a wide range of scores, with a subpopulation falling within the normative range of young adults, whereas others were impaired (Y, n = 7; AU, n = 9; AI, n = 7). In contrast to searching for the hidden platform, there was no statistical difference in cue training with a visible platform between the age groups (path length for young mean [SEM] = 217.14 [26.32] and for aged mean [SEM] = 296.47 [23.40], $t = 1.96$, $P > 0.05$).

GAD67-immunoreactive interneurons in hippocampal subfields of young and aged rats

The distribution and characteristics of GAD67 immunoreactivity in the young and aged hippocampus are illustrated in Figure 3. Total numbers of GAD67-immunoreactive neurons in each hippocampal subfield were derived using unbiased, design-based stereological methods. Figure 4 depicts the average number of GAD67-positive cell counts for young, AU, and AI rat groups in the DG, CA3, and CA1 subfields and sublayers within those regions. Although CA1 GAD67-positive neuron number remained stable across the adult rat life span (Fig. 4A,B), the DG and CA3 subfields exhibited an age-related decrease in the number of GAD67-immunopositive neurons (CA1, $F_{2,20} = 0.151$, $P = 0.860$; CA3, $F_{2,20} = 28.374$, $P < 0.001$, Y vs. AU and AI, $P < 0.001$; DG, $F_{2,20} = 18.788$, $P < 0.001$, Y vs. AU and AI, $P < 0.001$; Fig. 4C–F). This age-related loss in GAD67-positive neuron number was observed in all CA3 lamina and in both the moleculare and granule cell layers of the DG; totals included neuron counts from only the moleculare and granule cell layers and neuron counts from the hilus are considered separately below (CA3-SO, CA3-SP, CA3-SR, $P < 0.001$, Y vs. AU and AI, $P < 0.001$; CA3-SLM, $P < 0.05$, Y vs. AU and AI, $P < 0.05$; DG-GC, $P < 0.01$, Y vs. AU and AI, $P < 0.05$, DG-ML, $P < 0.01$, Y vs. AU and AI, $P < 0.01$).

Figure 5 depicts the total number of GAD67-positive and NeuN-immunoreactive neurons in the hilus of the DG. In contrast to the other hippocampal subregions and sublayers, GAD67-immunoreactive neuron loss in the hilus was linked to cognitive status among the aged rats, with reduced numbers of GAD67-positive hilar neurons observed selectively among aged rats with memory impairment ($F_{2,20} = 35.755$, $P < 0.001$; AI vs. Y and AU, $P < 0.001$; Y vs. AU, $P = 0.772$; Fig. 5A). Additionally, the number of GAD67-immunopositive hilar neurons was strongly associated with spatial memory among the aged individuals such that older rats with the lowest numbers of hilar GAD67-positive neurons exhibited the worst performance (N = 16, $r = -0.825$, $P = 0.001$; Fig. 5B). The reduction in GAD67-immunoreactive hilar neuron number is most apparent among AI rats and is represented in the photomicrographs in Figures 5 and 6. To determine whether the loss of GAD67-positive hilar neurons was associated with neuronal loss in the hilus, we also analyzed total neuron number in the dentate hilus using an antibody raised against the neuronal nuclei marker NeuN. Figure 5C shows the results, revealing no decline in the numbers of NeuN-positive hilar neurons ($F_{2,20} = 0.029$, $P = 0.971$; Fig. 5C,G–I).

NPY- and SOM-immunoreactive neuron counts in the hilus of the DG

To evaluate what specific interneuron subpopulations are most vulnerable under conditions of age-related cognitive impairment, we analyzed SOM- and NPY-immunoreactive interneuron number in the dentate hilus. As shown in Figure 7, our analysis of the dentate

hilus revealed a specific vulnerability of SOM-expressing hilar interneurons under conditions of age-related memory impairment. Aged rats with spatial memory deficits exhibited a significant decrease in SOM-positive hilar interneurons compared with young and AU rats, and the number of SOM-immunopositive hilar interneurons strongly correlated with spatial memory performance among the aged rats ($F_{2,20} = 37.922$, $P < 0.001$; AI vs. Y and AU, $P < 0.001$; Y vs. AU, $P = 0.806$; N = 16, r = −0.860, $P < 0.001$; Fig. 7A,B). The magnitude of SOM-positive hilar interneuron loss was approximately equal to the loss of GAD67-immunopositive hilar interneurons observed in AI rats, and the decline appears to involve, at least in part, an overlapping population that colocalizes both neurochemicals. Consistent with this interpretation, the numbers of GAD67- and SOM-immunoreactive hilar interneurons were highly correlated among the aged rats (N = 16, $r = 0.823$, $P < 0.001$). In contrast, NPY-positive hilar interneuron number remained stable across the adult rat life span regardless of cognitive status ($F_{2,20} = 0.051$, $P = 0.951$; Fig. 7C). Similar to the GAD67 hilar analysis, the reduction in SOM-immunoreactive hilar neuron number among AI rats was clearly evident, as illustrated in Figure 6D–F, although hilar NPY-positive neuron immunoreactivity appeared subjectively to be preserved (Fig. 6G – I).

SOM-immunoreactive neuron counts in CA3 stratum oriens

For comparison with the condition of hilar SOM-expressing interneurons in aging, we also examined SOM-expressing interneuron number in CA3 stratum oriens, a neuronal subtype that shares an arrangement of functional connectivity similar to SOM-positive interneurons in the dentate hilus. Known as the O-LM type cell, this interneuron subtype is innervated by CA3 pyramidal neurons and makes synaptic contact with pyramidal cell dendrites in stratum lacunosum-moleculare that receive perforant path input from entorhinal cortex layer II. The SOM-expressing interneuron subtype in CA3 stratum oriens is a prominent source of feedback inhibition to the CA3 region (Freund and Buzsaki, 1996). Similar to the age-related loss of GAD67-expressing interneurons reported above for CA3, SOM-expressing interneuron number was decreased in CA3 stratum oriens among the aged rats relative to young animals, independent of cognitive status ($F_{2,20} = 33.051$, $P < 0.001$; Y vs. AU and AI, $P < 0.001$; Fig. 7D).

SOM-immunoreactive neuron counts in the dentate hilus following levetiracetam treatment

Given that AI rats were observed to have a specific vulnerability in SOM-expressing hilar interneurons, we next tested whether SOM protein expression is restored by a drug treatment that we previously demonstrated ameliorates memory impairment in aged rats and in humans with aMCI (Bakker et al., 2012; Koh et al., 2010). Levetiracetam is a widely used antiepileptic agent that improves spatial memory function in aged Long-Evans rats with memory impairment. This treatment has also been shown to improve memory performance and reduce the dysfunctional condition of excess DG/CA3 activity in patients with aMCI (Bakker et al., 2012). Additionally, levetiracetam administration reduces both aberrant hippocampal activity and synaptic dysfunction and restores molecular markers in the dentate gyrus in an hAPPJ20 mouse model of Alzheimer’s disease (AD; Sanchez et al., 2012). In the current study, 4 weeks of low-dose levetiracetam administration (10 mg/kg/day) fully restored SOM expression among hilar interneurons in aged rats with documented memory deficits to levels comparable to those of young rats with intact memory (Fig. 8). AI rats that

received vehicle control infusion (saline) displayed significantly lower numbers of SOM-immunoreactive hilar neurons relative to either young and levetiracetam-treated aged rats (N = 18; $F_{2,20} = 15.739$, $P < 0.001$; AI-LEV vs. Y, $P = 0.679$; AI-LEV vs. AI-VEH, $P < 0.01$; AI-VEH vs. Y, $P < 0.001$), replicating the results reported above.

DISCUSSION

The current investigation assessed hippocampal GABAergic interneurons in aged rats with cognitive impairment, relative to aged cohorts and young adults with intact memory. The findings demonstrate a vulnerability affecting the hilus, with decreased numbers of GAD67- and SOM-positive neurons specifically observed in AI rats. No differences in those interneuron subpopulations were observed in comparisons of young adults and aged rats with preserved cognitive function. In addition, across the full spectrum of individual differences, the total numbers of hilar GAD67- and SOM-immunopositive interneurons correlated with memory performance among rats in the aged group such that those with the lowest numbers exhibited the greatest spatial memory impairment. Chronic administration of levetiracetam, a treatment that ameliorates memory impairment in cognitively impaired aged rats (Koh et al., 2010), restored SOM expression among hilar interneurons in AI rats. These data further suggest that SOM-positive hilar interneuron vulnerability contributes to the condition of age-related memory impairment.

Regional specificity in the loss of hippocampal interneuron integrity in aged rats with and without memory impairment

The selective decrease in number of GAD67-positive neurons in the hilus was a notable finding in this comprehensive examination across hippocampal subregions and laminae. In the CA1 subregion, GAD67-positive neurons remained stable independent of age and cognitive status. Aging, irrespective of cognitive status, was associated with reduced numbers of GAD67-immunoreactive interneurons in the CA3 and DG subfields, with similarly low interneuron counts across laminae making up the principal cell layers and connectional zones within those regions.

It is important to note that all SOM-expressing hilar interneurons colocalize GAD67 (Freund and Buzsaki, 1996; Houser, 2007). The current data show that the decline in SOM-expressing hilar interneurons accounted almost entirely for the magnitude of hilar GAD67-positive neuron loss observed in AI rats. This strongly suggests that hilar vulnerability under conditions of age-related cognitive impairment predominantly involves the GABAergic hilar interneurons that colocalize SOM. Notably, decreased numbers of hilar GAD67- and SOM-positive interneurons in aged rats with cognitive impairment were observed in the absence of changes in NeuN-positive neuron number. That finding is consistent with previous research with the Long-Evans rat model reporting a preservation of other neuronal populations throughout the hippocampal memory system, including principal neurons in the hippocampal formation and overall neuron counts in the parahippocampal regions of cortex (Rapp et al., 2002; Rapp and Gallagher, 1996). In the current context, the NeuN data suggest that decreased counts of GAD67- and SOM-positive hilar interneurons may be due to reduced protein expression rather than frank cell loss. That interpretation is consistent with

preserved numbers of hilar interneurons labeled for NPY immunoreactivity, an interneuron subtype overlapping with the affected GAD67- and SOM-positive populations. The restoration of SOM expression among hilar interneurons in AI rats treated with levetiracetam further indicates that the observed decrease in SOM-positive hilar neuron number is the result of reduced protein expression rather than frank neuron loss. It is important to recognize that immunohistochemical methods may not reliably label all GAD67-expressing neurons, and as a result the reported GAD67-positive cell counts may underestimate total interneuron number. Nonetheless, an underestimation in total interneuron number would not to detract from the findings of primary interest in the present study, documenting the reliable, regionally specific loss of interneuron integrity in aging, and specifically in aged animals with memory impairment (Table 3).

Potential impact of GAD67- and SOM-immunoreactive hilar interneuron number loss in AI rats

Decreased GAD67 and SOM protein expression may impact hilar interneuron function in AI rats. While other approaches would be needed to document fully the physiological consequences of hilar interneurons lacking GAD67 expression, evidence suggests that reduced levels of GAD67 protein expression would result in diminished functional inhibition. In support of this possibility, decreased levels of cytosolic GAD67 expression are associated with reduced GABA synthesis, diminished GABA release at the synapse, and decreased miniature inhibitory postsynaptic current amplitudes (mIPSCs) in cultured hippocampal neurons (Lau and Murthy, 2012). In addition, in aged rats studied by Stanley and colleagues (2012), diminished GAD67-immunopositive neuron number was coupled with reduced K^+/Ca^{2+}-evoked GABA release in the affected interneuron population.

Thus, a decline in somatic GAD67 expression can alter neuron function, and, in the context of age-related memory decline, altered hilar interneuron function could contribute to impairment in a signature computational processing capacity of the dentate gyrus. The ability to discriminate among similar experiences is a crucial feature of episodic memory. A role for the DG in pattern separation, by which similar inputs are encoded distinctively, has been attributed to the strongly divergent architecture of the DG, in which granule cells are tenfold more numerous than the cortical neurons that give rise to their principal innervation. Hilar interneurons have been suggested to contribute further to the sparse encoding mediated by granule cells in computational models (Freund and Buzsaki, 1996; Houser, 2007; Myers and Scharfman, 2009).

Empirical studies support a contribution of the hilus to the sparse encoding properties of granule cells in the DG. For example, increased granule cell excitability is observed in hippocampal slices following perforant path stimulation when hilar interneurons are ablated (Ratzliff et al., 2004). More recently, elevated granule cell firing rates together with increased numbers of cFos-positive neurons in the DG were observed when hilar GABAergic interneurons were silenced using in vivo optogenetic techniques (Andrews-Zwilling et al., 2012). Thus, increasing numbers of activated granule cells following hilar interneuron silencing would diminish the sparse encoding in DG required for optimal pattern separation. Consistent with a loss of such function, optogenetic inhibition of hilar

interneurons is sufficient to impair spatial learning and memory in mice (Andrews-Zwilling et al., 2012). Although the dentate hilus contains a functionally heterogeneous population of GABAergic interneurons, SOM-expressing hilar interneurons are uniquely positioned to maintain sparse encoding within the granule cell population via feedback inhibition onto granule cell dendrites in the perforant path termination zone (i.e., hilar perforant path-associated cell [HIPP cell]; Freund and Buzsaki, 1996; Houser, 2007; Myers and Scharfman, 2009). Accordingly, SOM-positive hilar interneuron vulnerability among aged rats with spatial memory impairment may contribute to the age-related pattern separation deficits previously reported for the Long-Evans rat model (Wilson et al., 2003, 2005b). Indeed, the restoration of SOM expression among hilar interneurons in AI rats following levetiracetam treatment reported here suggests that this hilar interneuron population plays an important role in modulating spatial memory function, which is dependent on pattern separation processes.

In the context of age-related cognitive impairment, it is also notable that SOM-expressing interneurons are one of the most vulnerable neuronal populations in AD (Davies et al., 1980; Kumar, 2005). For example, decreased numbers of SOM-positive hilar interneurons are observed in animal models of AD and under conditions of increased risk for AD (i.e., APOE4) that exhibit progressive decline in cognitive function with age (Andrews-Zwilling et al., 2010; Gordon et al., 2001; Ramos et al., 2006). Moreover, the severity of spatial learning impairment in apoE4 knock-in mice that exhibit accelerated age-dependent loss of hilar GABAergic interneurons is correlated with the extent of SOM-positive interneuron reduction (Andrews-Zwilling et al., 2010), an observation consistent with the current findings. Given the hypothesized role of the DG in memory processing, alterations affecting the hilar GABAergic network specifically related to SOM-positive HIPP cells may substantially contribute to the pattern separation failures observed in AD models (Palmer and Good, 2011).

Relationship between GAD67-positive neuron loss and other age-related alterations in the CA3 field

In contrast to the case in the hilus, GAD67- and SOM-positive interneurons located in CA3 stratum oriens were decreased in both AU and AI rats relative to young animals. Although the current data on the integrity of CA3 interneurons do not distinguish between the effects of aging with different cognitive outcomes, other measures within this region differentiate AI rats from those with preserved cognitive function. Such data include evidence of synapse loss affecting the perforant path input at CA3 distal dendrites only in AI rats and a CA3 mRNA expression profile in aging that distinguishes gene alterations related to chronological age from those associated with specific cognitive outcomes (Haberman et al., 2011; Smith et al., 2000). Thus, although decreased numbers of GAD67- and SOM-positive interneurons in CA3 are not specifically associated with age-related memory impairment, their decline may exacerbate the functional consequences of other CA3-specific alterations affecting AI rats.

Relevance of hilar interneuron vulnerability to the excess DG/CA3 activity observed in the aged, memory-impaired hippocampus

The current findings may be relevant to the origin of the excess DG/CA3 activity commonly observed when memory loss occurs in aging. Increased activity is found in the CA3 region in aged rats with cognitive impairment (Wilson et al., 2005a) and by high-resolution functional magnetic resonance imaging (fMRI) in the DG/CA3 regions of aged humans and patients diagnosed with aMCI (Yassa et al., 2010, 2011). Increased hippocampal activation has also been reported in individuals at risk for the development of AD (i.e., APOE4 allele carriers; Bassett et al., 2006; Bookheimer et al., 2000). Such excess activity in combination with other age-related hippocampal changes (i.e., loss of perforant path input) is proposed to shift the balance of computational functions of the entorhinal/DG/CA3 network from pattern separation to pattern completion, resulting in an inability to rapidly encode new information (Wilson et al., 2006). Our data are consistent with the possibility that a loss of inhibitory protein expression among interneurons in the dentate hilus contributes to the aberrant activity observed in the DG/CA3 network of older individuals and animals with memory impairment. Specifically, systemic administration of levetiracetam, an antiepileptic agent that at low doses improves memory in aged rats and in humans diagnosed with aMCI (Bakker et al., 2012; Koh et al., 2010), restored SOM protein expression among hilar interneurons in AI rats. These data suggest that restoring interneuron network function in the aged hippocampus may be therapeutically relevant to the amelioration of memory impairment and the condition of excess activity in some older individuals. Also supporting this hypothesis are data indicating that AI rats benefit from treatments designed to target a loss of GABAergic function in an effort to normalize activity, including transfection of an inhibitory neuropeptide into CA3 and administration of compounds that potentiate GABA at $GABA_A$ a5 receptors (Koh et al., 2010, 2013).

CONCLUSIONS

Results from the present study indicate that a loss in the number of hilar interneurons expressing GAD67 and SOM is associated with age-related memory impairment. The ability of levetiracetam treatment to rescue SOM expression among hilar interneurons suggests that vulnerability in this specific hilar interneuron subtype may contribute to the excess activity and encoding deficits previously reported for the AI Long-Evans rat (Wilson et al., 2006). Together, our data on the condition of hippocampal interneurons in relation to cognitive status with age further highlight the role that imbalances between excitatory and inhibitory functions in the hippocampus have in age-related memory decline.

Acknowledgments

Grant sponsor: National Institute on Aging; Grant number: P01AG009973-18 (to M.G.); Grant sponsor: Intramural Research Program of the National Institute on Aging..

LITERATURE CITED

Andrews-Zwilling Y, Bien-Ly N, Xu Q, Li G, Bernardo A, Yoon SY, Zwilling D, Yan TX, Chen L, Huang Y. Apolipoprotein E4 causes age- and tau-dependent impairment of GABAergic

interneurons, leading to learning and memory deficits in mice. J Neurosci. 2010; 30:13707–13717. [PubMed: 20943911]

Andrews-Zwilling Y, Gillespie AK, Kravitz AV, Nelson AB, Devidze N, Lo I, Yoon SY, Bien-Ly N, Ring K, Zwilling D, Potter GB, Rubenstein JL, Kreitzer AC, Huang Y. Hilar GABAergic interneuron activity controls spatial learning and memory retrieval. PLoS One. 2012; 7:e40555. [PubMed: 22792368]

Bakker A, Krauss GL, Albert MS, Speck CL, Jones LR, Stark CE, Yassa MA, Bassett SS, Shelton AL, Gallagher M. Reduction of hippocampal hyperactivity improves cognition in amnestic mild cognitive impairment. Neuron. 2012; 74:467–474. [PubMed: 22578498]

Bassett SS, Yousem DM, Cristinzio C, Kusevic I, Yassa MA, Caffo BS, Zeger SL. Familial risk for Alzheimer's disease alters fMRI activation patterns. Brain. 2006; 129:1229–1239. [PubMed: 16627465]

Baxter MG, Gallagher M. Neurobiological substrates of behavioral decline: models and data analytic strategies for individual differences in aging. Neurobiol Aging. 1996; 17:491–495. [PubMed: 8725914]

Bookheimer SY, Strojwas MH, Cohen MS, Saunders AM, Pericak-Vance MA, Mazziotta JC, Small GW. Patterns of brain activation in people at risk for Alzheimer's disease. N Engl J Med. 2000; 343:450–456. [PubMed: 10944562]

Davies P, Katzman R, Terry RD. Reduced somatostatin-like immunoreactivity in cerebral cortex from cases of Alzheimer disease and Alzheimer senile dementa. Nature. 1980; 288:279–280. [PubMed: 6107862]

Fetissov SO, Bensing S, Mulder J, Le Maitre E, Hulting AL, Harkany T, Ekwall O, Skoldberg F, Husebye ES, Perheentupa J, Rorsman F, Kampe O, Hokfelt T. Autoantibodies in autoimmune polyglandular syndrome type I patients react with major brain neurotransmitter systems. J Comp Neurol. 2009; 513:1–20. [PubMed: 19107747]

Fong AY, Stornetta RL, Foley CM, Potts JT. Immunohistochemical localization of GAD67-expressing neurons and processes in the rat brainstem: subregional distribution in the nucleus tractus solitarius. J Comp Neurol. 2005; 493:274–290. [PubMed: 16255028]

Freund TF, Buzsaki G. Interneurons of the hippocampus. Hippocampus. 1996; 6:347–470. [PubMed: 8915675]

Gallagher M, Burwell R, Burchinal M. Severity of spatial learning impairment in aging: development of a learning index for performance in the Morris water maze. Behav Neurosci. 1993; 107:618–626. [PubMed: 8397866]

Gavilan MP, Revilla E, Pintado C, Castano A, Vizuete ML, Moreno-Gonzalez I, Baglietto-Vargas D, Sanchez-Varo R, Vitorica J, Gutierrez A, Ruano D. Molecular and cellular characterization of the age-related neuroinflammatory processes occurring in normal rat hippocampus: potential relation with the loss of somatostatin GABAergic neurons. J Neurochem. 2007; 103:984–996. [PubMed: 17666053]

Gordon MN, King DL, Diamond DM, Jantzen PT, Boyett KV, Hope CE, Hatcher JM, DiCarlo G, Gottschall WP, Morgan D, Arendash GW. Correlation between cognitive deficits and Abeta deposits in transgenic APP 1 PS1 mice. Neurobiol Aging. 2001; 22:377–385. [PubMed: 11378242]

Haberman RP, Colantuoni C, Stocker AM, Schmidt AC, Pedersen JT, Gallagher M. Prominent hippocampal CA3 gene expression profile in neurocognitive aging. Neurobiol Aging. 2011; 32:1678–1692. [PubMed: 19913943]

Halabisky B, Parada I, Buckmaster PS, Prince DA. Excitatory input onto hilar somatostatin interneurons is increased in a chronic model of epilepsy. J Neurophysiol. 2010; 104:2214–2223. [PubMed: 20631216]

Hattiangady B, Rao MS, Shetty GA, Shetty AK. Brain-derived neurotrophic factor, phosphorylated cyclic AMP response element binding protein and neuropeptide Y decline as early as middle age in the dentate gyrus and CA1 and CA3 subfields of the hippocampus. Exp Neurol. 2005; 195:353–371. [PubMed: 16002067]

Houser CR. Interneurons of the dentate gyrus: an overview of cell types, terminal fields and neurochemical identity. Prog Brain Res. 2007; 163:217–232. [PubMed: 17765721]

Koh MT, Haberman RP, Foti S, McCown TJ, Gallagher M. Treatment strategies targeting excess hippocampal activity benefit aged rats with cognitive impairment. Neuropsychopharmacology. 2010; 35:1016–1025. [PubMed: 20032967]

Koh MT, Rosenzweig-Lipson S, Gallagher M. Selective $GABA_A$ alpha5 positive allosteric modulators improve cognitive function in aged rats with memory impairment. Neuropharmacology. 2013; 64:145–152. [PubMed: 22732440]

Kumar U. Expression of somatostatin receptor subtypes (SSTR1-5) in Alzheimer's disease brain: an immunohistochemical analysis. Neuroscience. 2005; 134:525–538. [PubMed: 15961235]

Lau CG, Murthy VN. Activity-dependent regulation of inhibition via GAD67. J Neurosci. 2012; 32:8521–8531. [PubMed: 22723692]

Maei HR, Zaslavsky K, Teixeira CM, Frankland PW. What is the most sensitive measure of water maze probe test performance? Front Integr Neurosci. 2009; 3:4. [PubMed: 19404412]

Mullen RJ, Buck CR, Smith AM. NeuN, a neuronal specific nuclear protein in vertebrates. Development. 1992; 116:201–211. [PubMed: 1483388]

Myers CE, Scharfman HE. A role for hilar cells in pattern separation in the dentate gyrus: a computational approach. Hippocampus. 2009; 19:321–337. [PubMed: 18958849]

Palmer A, Good M. Hippocampal synaptic activity, pattern separation and episodic-like memory: implications for mouse models of Alzheimer's disease pathology. Biochem Soc Trans. 2011; 39:902–909. [PubMed: 21787321]

Paxinos, G.; Watson, C. The rat brain in stereotaxic coordinates, compact. 3rd. San Diego: Academic Press; 1997.

Ramos B, Baglietto-Vargas D, del Rio JC, Moreno-Gonzalez I, Santa-Maria C, Jimenez S, Caballero C, Lopez-Tellez JF, Khan ZU, Ruano D, Gutierrez A, Vitorica J. Early neuropathology of somatostatin/NPY GABAergic cells in the hippocampus of a PS1 3 APP transgenic model of Alzheimer's disease. Neurobiol Aging. 2006; 27:1658–1672. [PubMed: 16271420]

Rapp PR, Gallagher M. Preserved neuron number in the hippocampus of aged rats with spatial learning deficits. Proc Natl Acad Sci U S A. 1996; 93:9926–9930. [PubMed: 8790433]

Rapp PR, Deroche PS, Mao Y, Burwell RD. Neuron number in the parahippocampal region is preserved in aged rats with spatial learning deficits. Cereb Cortex. 2002; 12:1171–1179. [PubMed: 12379605]

Ratzliff, AdH; Howard, AL.; Santhakumar, V.; Osapay, I.; Soltesz, I. Rapid deletion of mossy cells does not result in a hyperexcitable dentate gyrus: implications for epileptogenesis. J Neurosci. 2004; 24:2259–2269. [PubMed: 14999076]

Real MA, Heredia R, Labrador Mdel C, Davila JC, Guirado S. Expression of somatostatin and neuropeptide Y in the embryonic, postnatal, and adult mouse amygdalar complex. J Comp Neurol. 2009; 513:335–348. [PubMed: 19177517]

Ruscheweyh R, Forsthuber L, Schoffnegger D, Sandkuhler J. Modification of classical neurochemical markers in identified primary afferent neurons with Abeta-, Adelta-, and C-fibers after chronic constriction injury in mice. J Comp Neurol. 2007; 502:325–336. [PubMed: 17348016]

Sanchez PE, Zhu L, Verret L, Vossel KA, Orr AG, Cirrito JR, Devidze N, Ho K, Yu GQ, Palop JJ, Mucke L. Levetiracetam suppresses neuronal network dysfunction and reverses synaptic and cognitive deficits in an Alzheimer's disease model. Proc Natl Acad Sci U S A. 2012; 109:E2895–E2903. [PubMed: 22869752]

Shetty AK, Turner DA. Hippocampal interneurons expressing glutamic acid decarboxylase and calcium-binding proteins decrease with aging in Fischer 344 rats. J Comp Neurol. 1998; 394:252–269. [PubMed: 9552130]

Shi L, Argenta AE, Winseck AK, Brunso-Bechtold JK. Stereological quantification of GAD-67-immunoreactive neurons and boutons in the hippocampus of middle-aged and old Fischer 344 3 brown Norway rats. J Comp Neu-rol. 2004; 478:282–291.

Singec I, Knoth R, Ditter M, Volk B, Frotscher M. Neurogranin is expressed by principal cells but not interneurons in the rodent and monkey neocortex and hippocampus. J Comp Neurol. 2004; 479:30–42. [PubMed: 15389613]

Smith TD, Adams MM, Gallagher M, Morrison JH, Rapp PR. Circuit-specific alterations in hippocampal synaptophysin immunoreactivity predict spatial learning impairment in aged rats. J Neurosci. 2000; 20:6587–6593. [PubMed: 10964964]

Stanley DP, Shetty AK. Aging in the rat hippocampus is associated with widespread reductions in the number of glutamate decarboxylase-67 positive interneurons but not interneuron degeneration. J Neurochem. 2004; 89:204–216. [PubMed: 15030405]

Stanley EM, Fadel JR, Mott DD. Interneuron loss reduces dendritic inhibition and GABA release in hippocampus of aged rats. Neurobiol Aging. 2012; 33:431. [PubMed: 21277654]

Stranahan AM, Jiam NT, Stocker AM, Gallagher M. Aging reduces total neuron number in the dorsal component of the rodent prefrontal cortex. J Comp Neurol. 2012; 520:1318–1326. [PubMed: 22020730]

Sun C, Mtchedlishvili Z, Bertram EH, Erisir A, Kapur J. Selective loss of dentate hilar interneurons contributes to reduced synaptic inhibition of granule cells in an electrical stimulation-based animal model of temporal lobe epilepsy. J Comp Neurol. 2007; 500:876–893. [PubMed: 17177260]

Vezzani A, Schwarzer C, Lothman EW, Williamson J, Sperk G. Functional changes in somatostatin and neuropeptide Y containing neurons in the rat hippocampus in chronic models of limbic seizures. Epilepsy Res. 1996; 26:267–279. [PubMed: 8985706]

West MJ. Regionally specific loss of neurons in the aging human hippocampus. Neurobiol Aging. 1993; 14:287–293. [PubMed: 8367010]

West MJ, Slomianka L, Gundersen HJ. Unbiased stereological estimation of the total number of neurons in the subdivisions of the rat hippocampus using the optical fractionator. Anat Rec. 1991; 231:482–497. [PubMed: 1793176]

Wilson IA, Ikonen S, McMahan RW, Gallagher M, Eichenbaum H, Tanila H. Place cell rigidity correlates with impaired spatial learning in aged rats. Neurobiol Aging. 2003; 24:297–305. [PubMed: 12498963]

Wilson IA, Ikonen S, Gallagher M, Eichenbaum H, Tanila H. Age-associated alterations of hippocampal place cells are subregion specific. J Neurosci. 2005a; 25:6877–6886. [PubMed: 16033897]

Wilson IA, Ikonen S, Gurevicius K, McMahan RW, Gallagher M, Eichenbaum H, Tanila H. Place cells of aged rats in two visually identical compartments. Neurobiol Aging. 2005b; 26:1099–1106. [PubMed: 15748790]

Wilson IA, Gallagher M, Eichenbaum H, Tanila H. Neurocognitive aging: prior memories hinder new hippocampal encoding. Trends Neurosci. 2006; 29:662–670. [PubMed: 17046075]

Yassa MA, Stark SM, Bakker A, Albert MS, Gallagher M, Stark CE. High-resolution structural and functional MRI of hippocampal CA3 and dentate gyrus in patients with amnestic mild cognitive impairment. Neuroimage. 2010; 51:1242–1252. [PubMed: 20338246]

Yassa MA, Lacy JW, Stark SM, Albert MS, Gallagher M, Stark CE. Pattern separation deficits associated with increased hippocampal CA3 and dentate gyrus activity in nondemented older adults. Hippocampus. 2011; 21:968–979. [PubMed: 20865732]

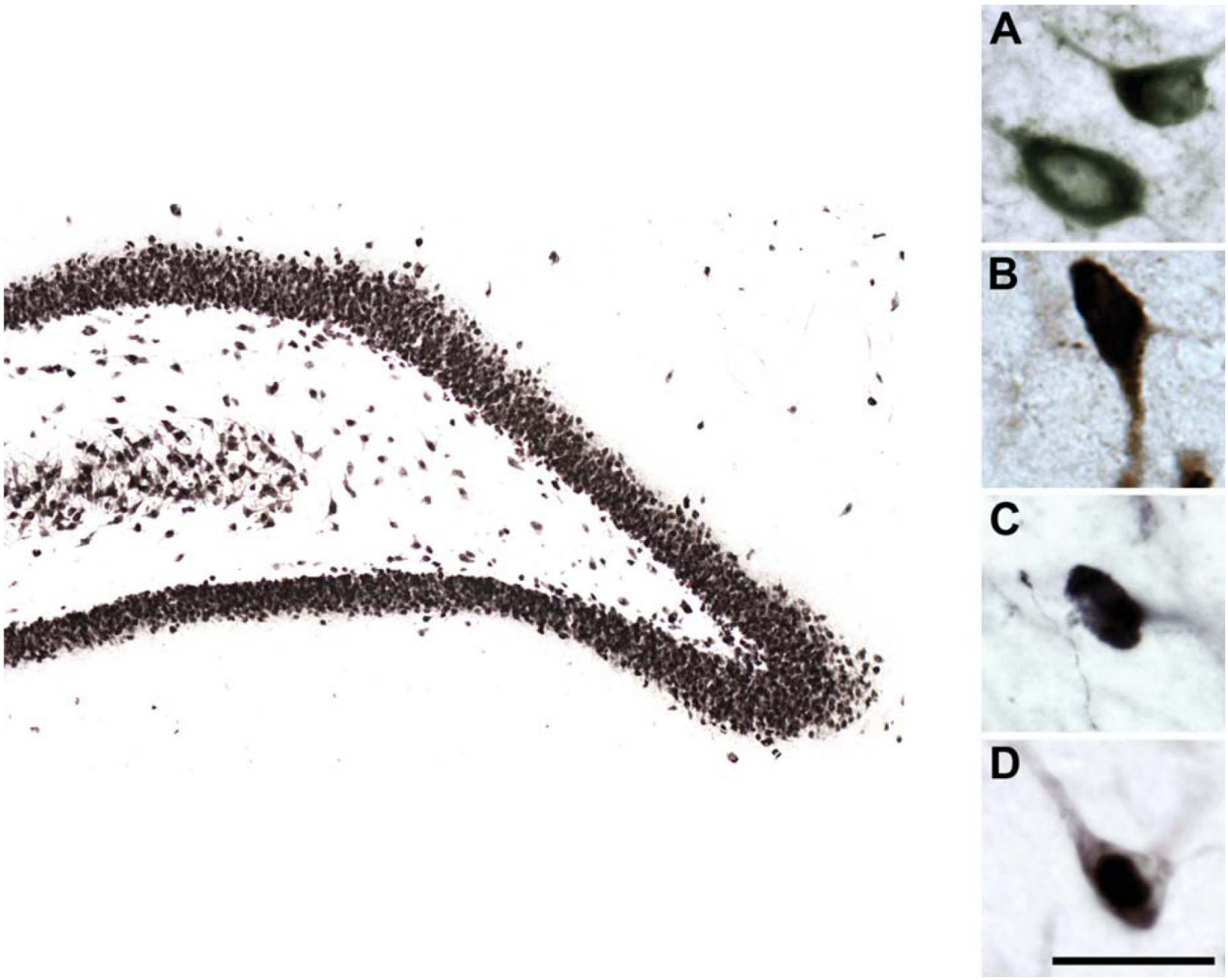

Figure 1.

High-magnification photomicrographs of GAD67-, SOM-, NPY-, and NeuN-immunoreactive hilar neurons. Representative GAD67 (**A**)-, SOM (**B**)-, NPY (**C**)-, and NeuN (**D**)-immunoreactive hilar neurons viewed at high magnification. Larger image depicts NeuN-immunoreactive neurons in the dentate gyrus. Scale bar = 25 μm in D (applies to A–D); 200 μm for larger image.

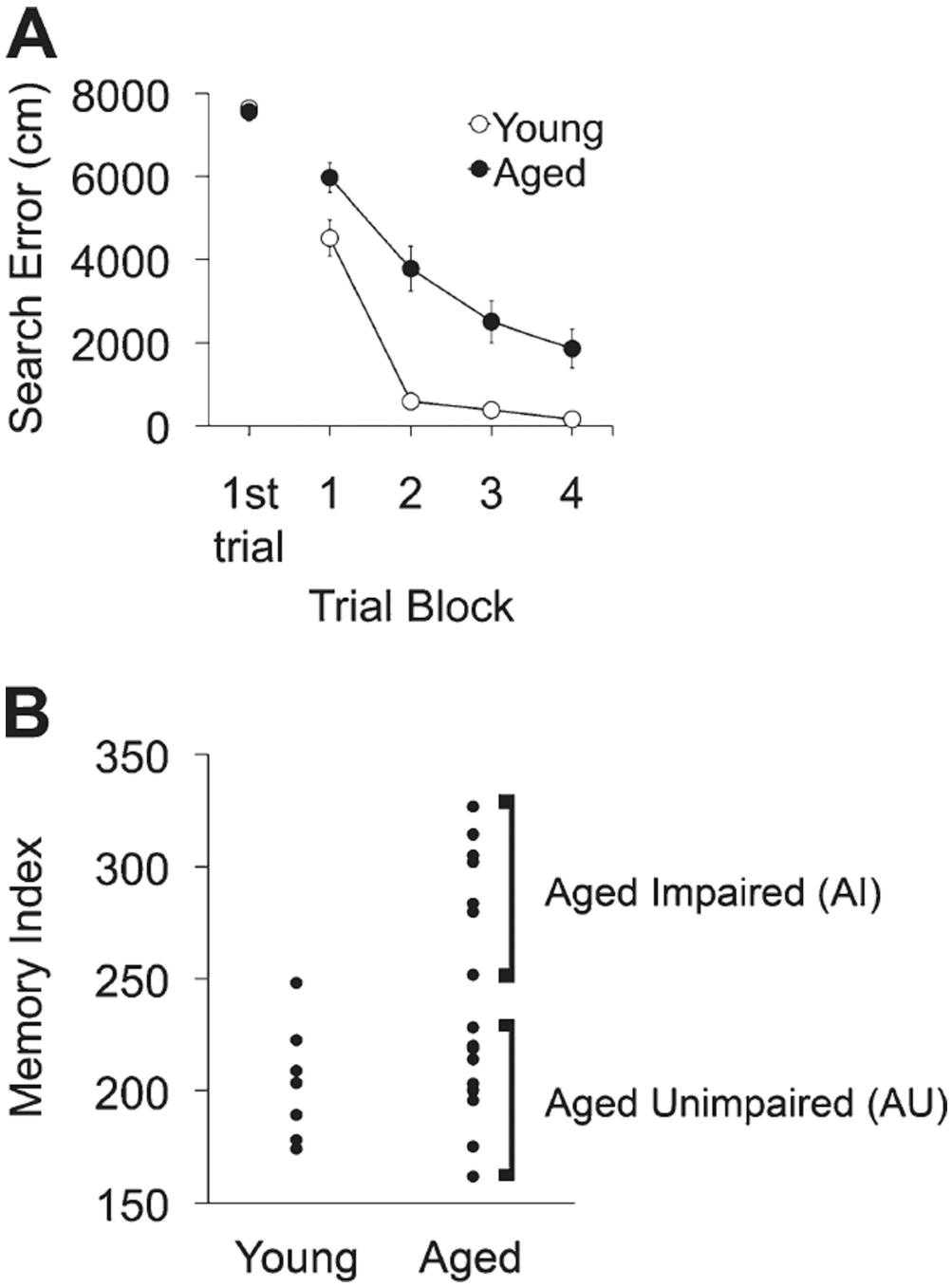

Figure 2.

Behavioral assessment of young and aged male Long-Evans rats in the spatial water maze. **A**: Cumulative search error across five blocks of training trials using a measure of proximity to the escape platform throughout the search. This assessment revealed impairment in spatial learning in aged rats relative to young; however, search on the initial learning trial was equivalent between the two groups. **B**: Memory index score of spatial bias during probe trial swimming. This measure reflects the average proximity to the escape platform location (platform retracted) across interpolated probe trials. Lower scores represent a more accurate

search and better memory function than higher scores. As a group aged rats exhibited memory impairment on this task, but some aged rats performed within the normative range of the young and were characterized as aged unimpaired (AU). Those rats performing outside the range of young animals were characterized as aged impaired (AI). Error bars represent ± SEM.

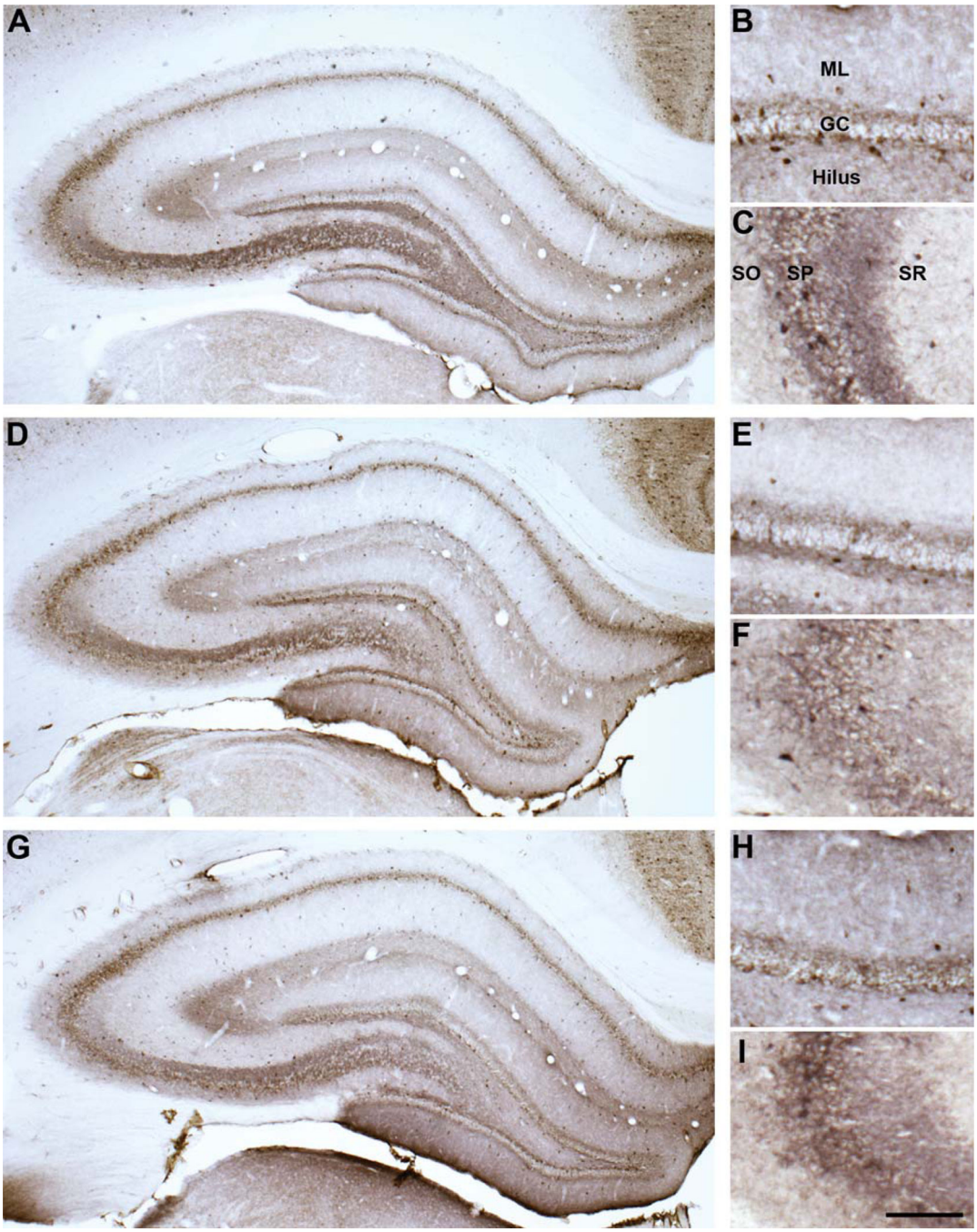

Figure 3.

Representative GAD67 hippocampal immunoreactivity. GAD67 immunoreactivity in young (**A–C**), aged memory-unimpaired (**D–F**), and aged memory-impaired (**G–I**) rats in the hippocampus (A,D,G), dentate gyrus (B,E,H), and CA3 (C,F,I). GAD67, glutamic acid decarboxylase-67; GC, dentate granule cell layer; ML, dentate moleculare layer; SO, stratum oriens; SP, stratum pyramidal; SR, stratum radiatum. Scale bar = 150 μm (applies to B,C,E,F,H,I); 400 μm (apples to A,D,G).

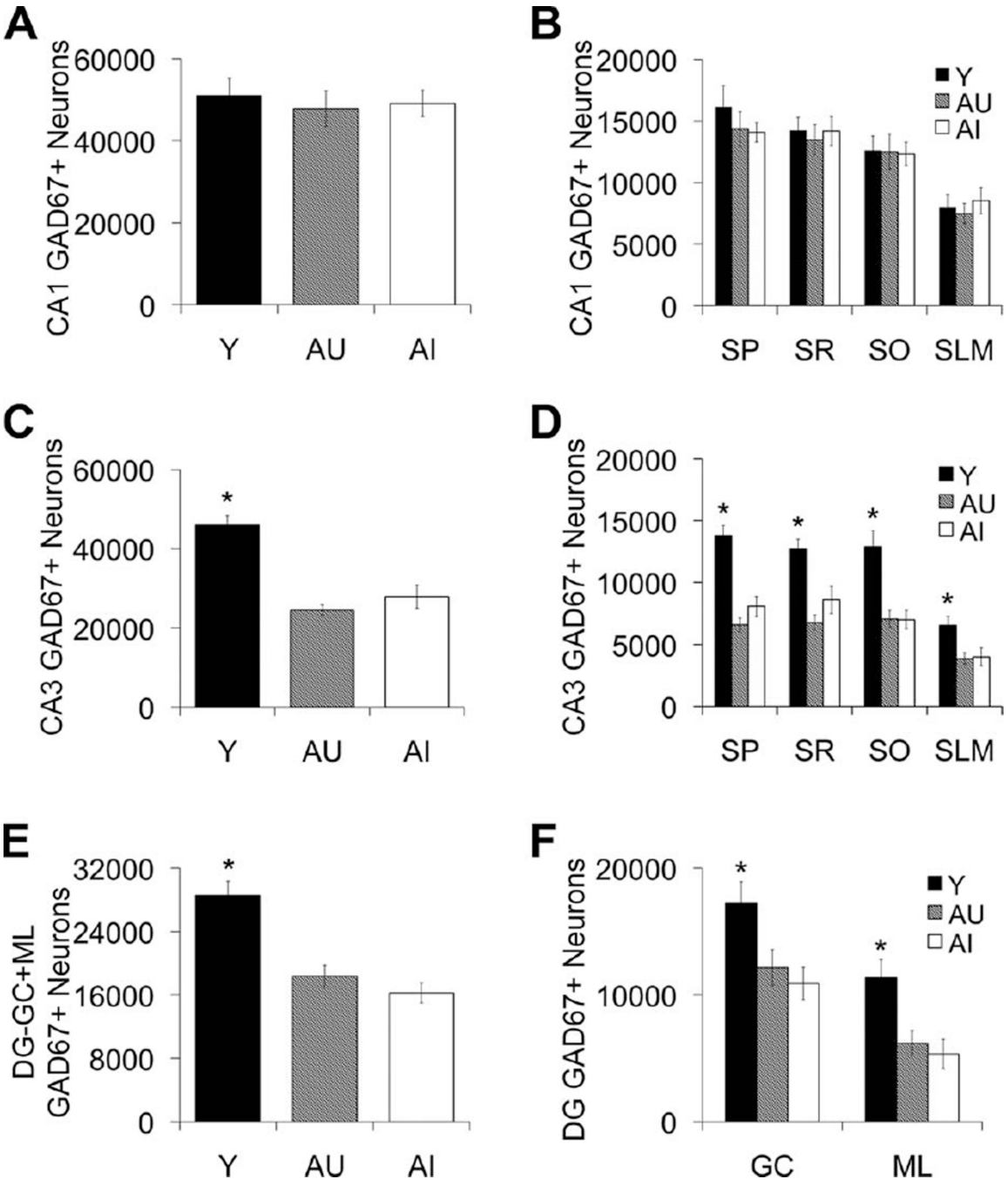

Figure 4.

GAD67-positive interneuron counts in hippocampal subfields CA1, CA3, and DG. **A,B**: Number of CA1 GAD67-positive neurons remains stable across the adult rat life span regardless of cognitive status. **C,D**: GAD67-positive neurons are reduced in AU and AI rats in the CA3 hippocampal subregion. **E,F**: GAD67-positive neurons are reduced in AU and AI rats in the DG moleculare (ML) and granule cell (GC) layers. Numbers of GAD67-positive neurons in the dentate hilus are depicted in Figure 5A,B. Error bars represent ± SEM. Y, young; AU, aged unimpaired; AI, aged impaired; GAD67, glutamic acid

decarboxylase-67; SP, stratum pyramidal; SR, stratum radiatum; SO, stratum oriens; SLM, stratum lacunosum-moleculare. *$P < 0.05$.

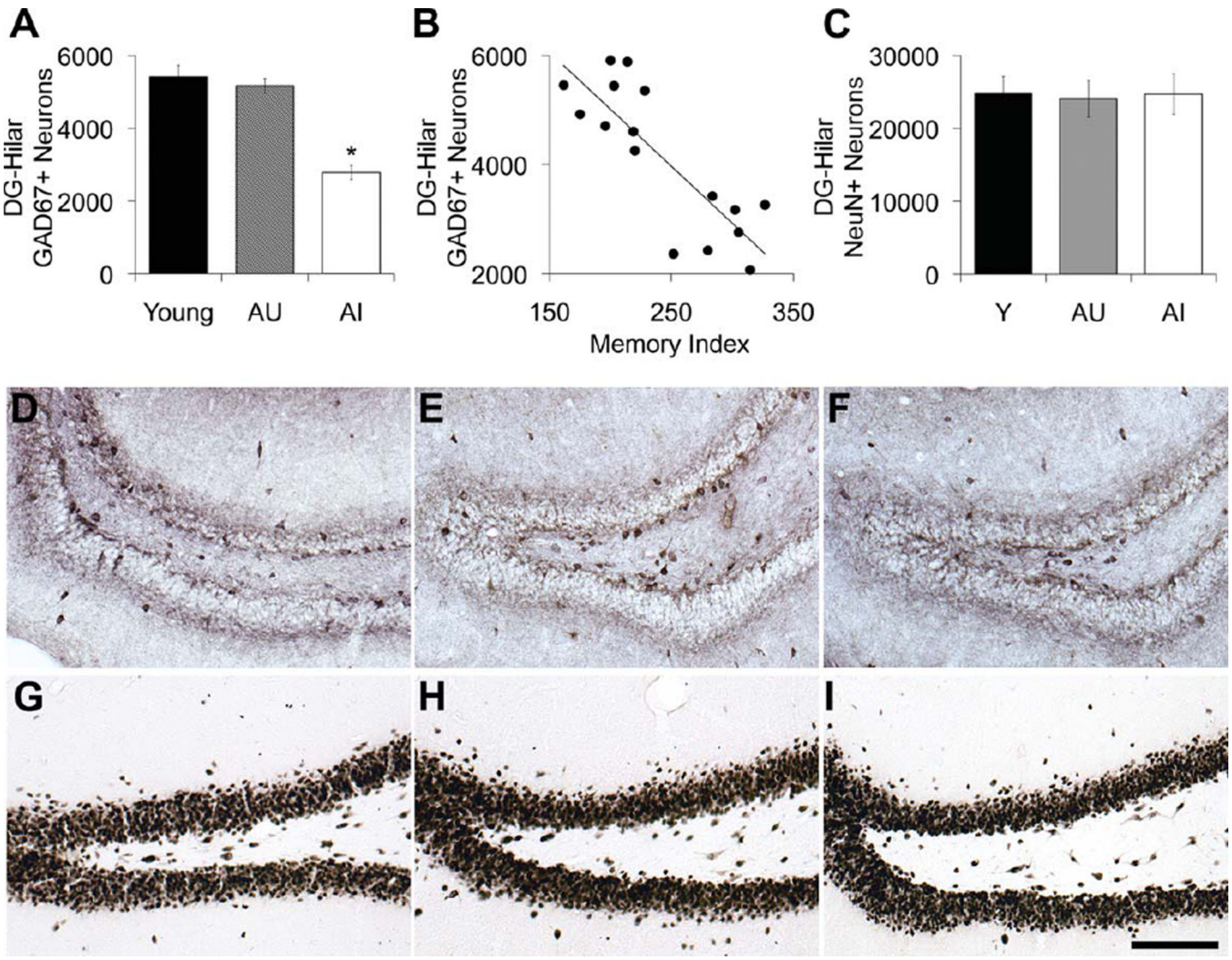

Figure 5.

GAD67-positive and NeuN-positive neuron counts in the dentate hilus. **A**: Number of GAD67-positive neurons is reduced in the hilus of AI rats relative to young and AU rat groups. **B**: The number of GAD67-positive neurons in the dentate hilus correlates with spatia memory function among the aged rat cohorts (AU and AI), $r = -0.825$, $P < 0.01$. **C**: Number of NeuN-positive neurons in the hilus remains stable across the adult rat life span regardless of cognitive status. **D–F**: Representative immunohistochemical staining of GAD67 abeled neurons in the dentate hilus of young (D), AU (E), and AI (F) rats. GAD67-immunopositive neurons are visibly reduced in AI rats. **G–l**: Representative immunohistochemical staining of NeuN-labeled neurons in the dentate hilus of young (G), AU (H), and AI (I) rats. Error bars represent ± SEM. Y, young; AU, aged unimpaired; AI aged impaired; GAD67, glutamic acid decarboxylase-67; NeuN, neuronal nuclei protein. *$P < 0.001$. Scale bar = 100 μm.

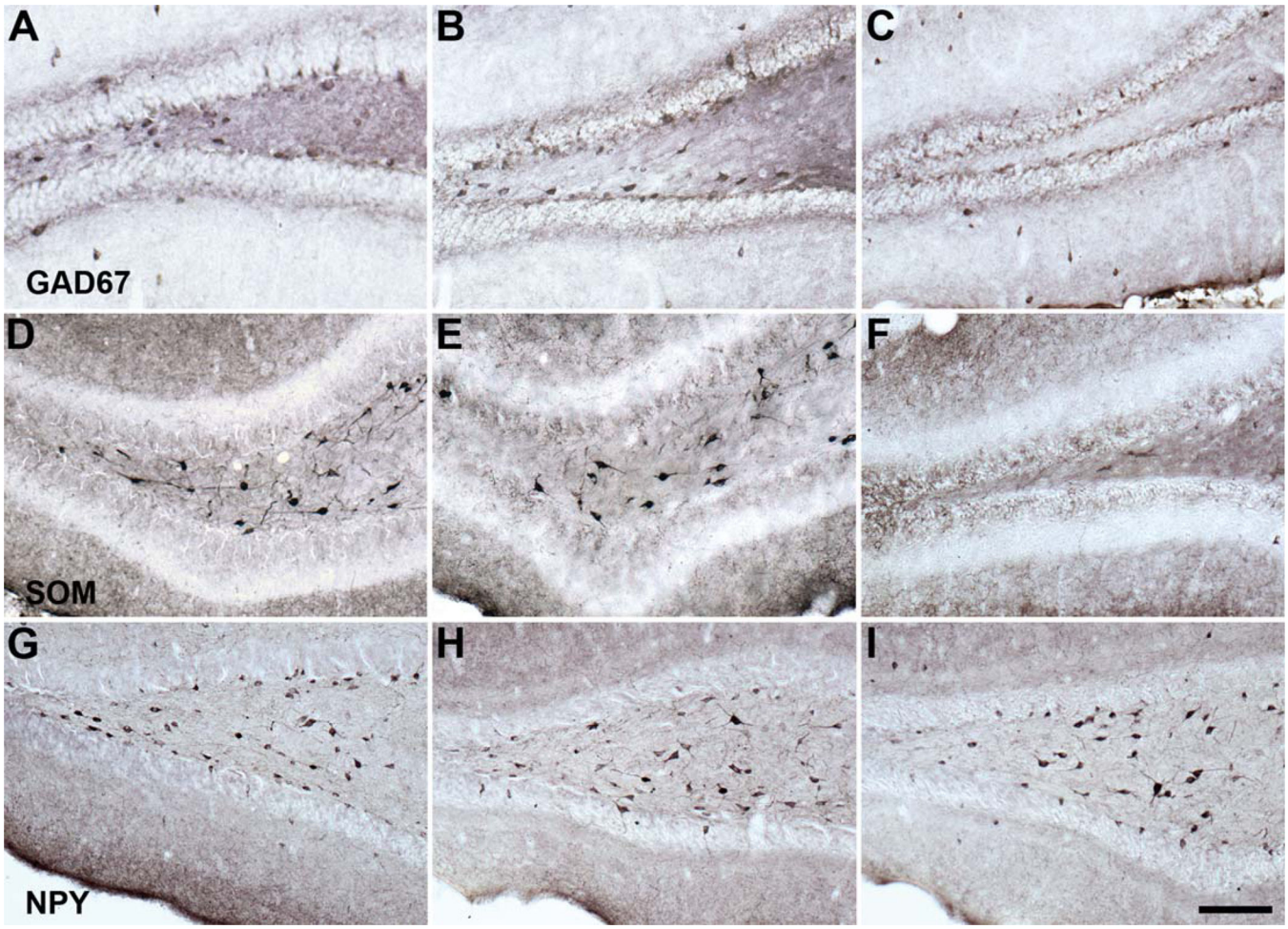

Figure 6.

Representative GAD67, SOM, and NPY immunoreactivity in the young and old rat dentate hilus. **A–C**: Hilar GAD67 immunoreactivity in the young (A), aged memory-unimpaired (B), and aged memory-impaired (C) rats. **D–F**: Hilar SOM immunoreactivity in the young (D), aged memory-unimpaired (E), and aged memory-impaired (F) rat. **G–I**: Hilar NPY immunoreactivity in the young (G), aged memory-unimpaired (H), and aged memory-impaired (I) rat. GAD67, glutamic acid decarboxylase-67; SOM, somatostatin; NPY, neuropeptide Y. Scale bar = 100 μm.

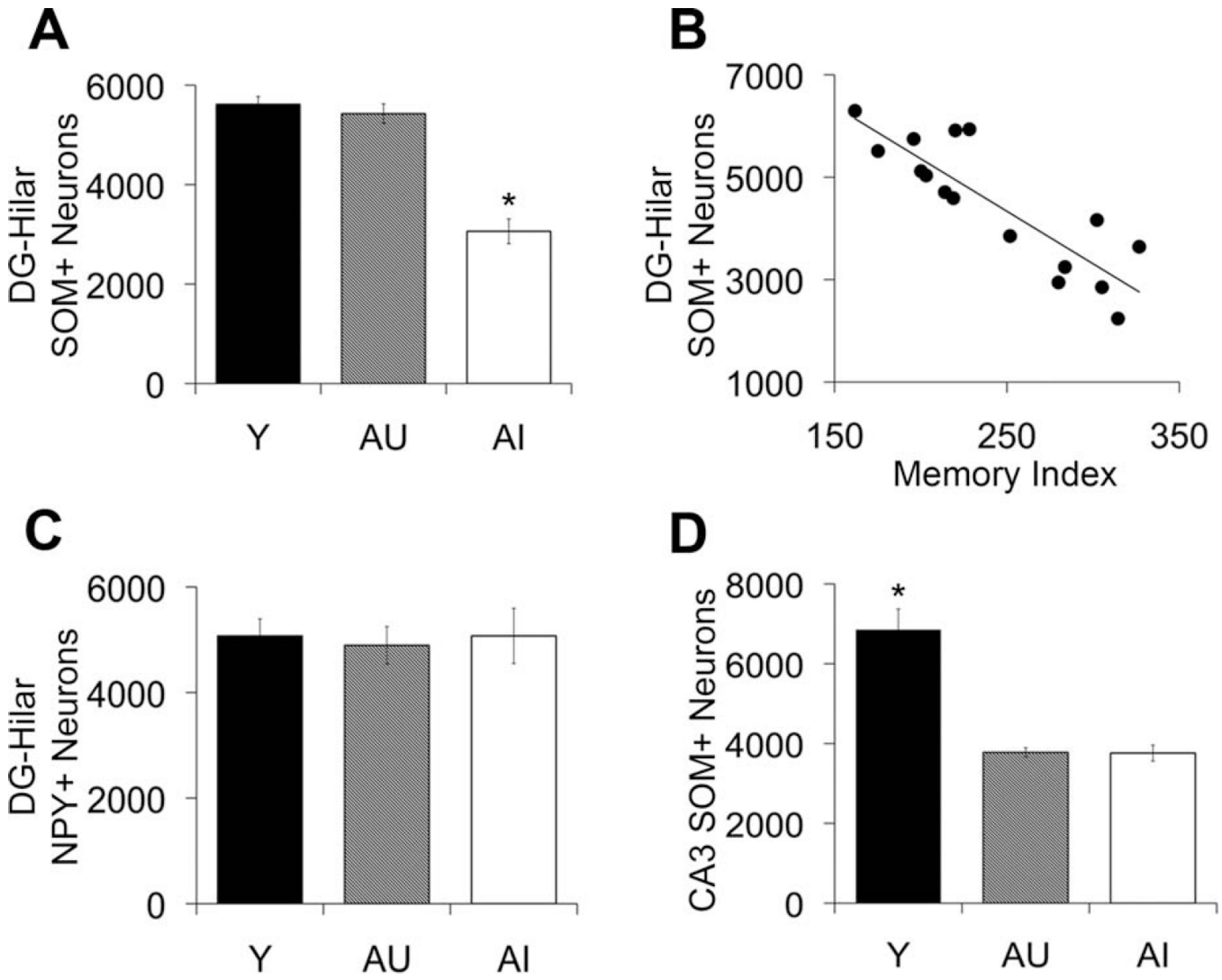

Figure 7.

SOM-positive and NPY-positive neuron counts in the dentate hilus and CA3 stratum oriens. **A**: Number of SOM-positive neurons in the dentate hilus is reduced in AI rats relative to young and AU animals. **B**: Number of SOM-positive neurons in the dentate hilus correlates with spatial memory function among the aged rat cohorts, $r = 20.860$, $P < 0.001$. **C**: Number of NPY-positive neurons in the hilus remains stable across the adult rat life span regardless of cognitive status. **D**: Number of SOM-positive neurons is reduced in CA3 stratum oriens of AU and AI rats relative to young. Error bars represent ± SEM. Y, young; AU, aged unimpaired; AU aged impaired; NPY, neuropeptide Y; SOM, somatostatin. *$P < 0.001$.

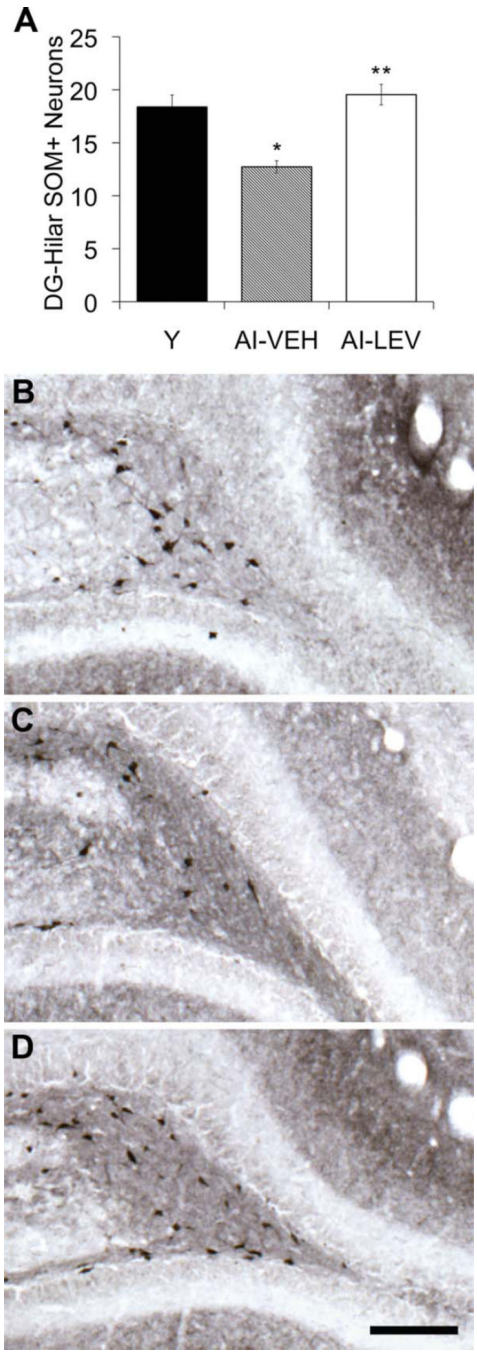

Figure 8.

SOM-positive neuron counts in the dentate hilus of evetiracetam-treated rats. **A**: SOM-positive neuron counts in the dentate hilus were lower in the AI-VEH rat group compared with young rats. Levetiracetam treatment increased SOM-positive neuron counts in AI-LEV rats relative to AI-VEH (Y = 18.4, SEM ± 1.12; AI-VEH = 12.7, SEM ± 0.58; AI-LEV = 19.5, SEM ± 0.97). **B–D**: Hilar SOM immunoreactivity in the dentate hilus of young (B), AI-VEH (C), and AI-LEV (D) rats. Error bars represent ± SEM. Y, young; AI-VEH,

vehicle-treated aged impaired; AI-LEV, levetiracetam-treated aged impaired; SOM, somatostatin. *$P < 0.001$, **$P < 0.01$. Scale bar = 150 μm.

TABLE 1

Primary Antibody Information[1]

Antigen	Immunizing antigen	Manufacturer details	Dilution
Glutamic acid decaboxylase-67 (GAD67)	Recombinant GAD67 protein corresponding to amino acids 4–10 of human GAD67	Chemicon (Millipore), catalog No. MAB5406, mouse monoclonal	1:1,000
Neuronal nuclear protein (NeuN)	Cell nuclei purified from mouse brain	Chemicon (Millipore), catalog No. MAB377, mouse monoclonal	1:10,000
Neuropeptide Y (NPY)	Synthetic porcine peptide (whole molecule) conjugated to KLH	Sigma-Aldrich, catalog No. N9528, rabbit polyclonal	1:4,000
Somatostatin (SOM)	Synthetic peptide LELQRSANSNPAMAPRERK corresponding to amino acids 84–102 of human SOM	Santa Cruz Biotechnology, catalog No. SC7819, goat polyclonal	1:400

[1]Concentrations listed indicate the optimal antibody dilutions used in each experiment.

TABLE 2

Stereological Sampling Parameters for Analysis of Interneuron Cell Counts and Total Neuron Number in Young and Aged Rats[1]

	GAD67				SOM			
Subregion	**CA1**	**CA3**	**DG**	**Hilus**	**Hilus**	**CA3-SO**	**NPY (hilus)**	**NeuN (hilus)**
X-step size (μm)	150	150	150	50	50	75	50	50
Y-step size (μm)	150	150	150	50	50	75	50	50
Disector volume (μm^3)	35,000	35,000	35,000	35,000	22,500	22,500	22,500	5,625
Counting frame area (μm^2)	2,500	2,500	2,500	2,500	2,500	2,500	2,500	625
				Number of sections				
Young	10 (0.26)	10 (0.14)	11 (0.36)	11 (0.37)	11 (0.46)	10 (0.14)	10 (0.20)	10 (0.20)
AU	10 (0.15)	10 (0.17)	11 (0.17)	10 (0.31)	10 (0.42)	10 (0.17)	11 (0.40)	10 (0.24)
AI	11 (0.14)	10 (0.14)	11 (0.34)	10 (0.53)	10 (0.44)	10 (0.26)	10(0.36)	11 (0.26)
				Section thickness (μm)				
Young	21 (0.39)	22 (0.87)	22 (0.39)	21 (0.28)	13 (0.09)	14 (0.21)	14 (0.47)	13 (0.09)
AU	21 (0.53)	22 (0.42)	21 (0.45)	21 (0.52)	13 (0.23)	14 (0.35)	14 (0.34)	14 (0.10)
AI	21 (0.65)	22 (0.80)	22 (0.52)	21 (0.62)	14 (0.21)	14 (0.32)	15 (0.12)	13 (0.11)
				Coefficient of error				
Young	0.08 (0.001)	0.08 (0.007)	0.09 (0.001)	0.07 (0.003)	0.07 (0.005)	0.07 (0.003)	0.06 (0.003)	0.09 (0.004)
AU	0.08 (0.001)	0.11 (0.006)	0.11 (0.004)	0.07 (0.002)	0.08 (0.004)	0.10 (0.003)	0.06 (0.003)	0.09 (0.003)
AI	0.08 (0.002)	0.11 (0.007)	0.11 (0.002)	0.10 (0.005)	.08 (0.006)	0.10 (0.004)	0.06 (0.003)	0.09 (0.004)

[1]Values represent the group mean with the standard error of the mean in parenthesis. GAD67, glutamic acid decarboxylase-67; SOM, somatostatin; NPY, neuropeptide Y; NeuN, neuronal nuclei protein; DG, dentate gyrus; SO, stratum oriens; SP, stratum pyramidal; SR, stratum radiatum; SLM, stratum lacunosum-moleculare; GC, granule cell layer; ML, molecular cell layer.

TABLE 3

Total Estimated Numbers of Hippocampal and Hilar Neurons Immunoreactive for GAD67, NeuN, SOM, and NPY[1]

Marker/region	Young	AU	Al
	GAD67/CA1		
Total	50,987 (4,293)	47,869 (4,273)	49,120 (3,246)
SO	12,623 (1,147)	12,509 (1,366)	12,322 (948)
SP	16,139 (1,734)	14,356 (1,427)	14,073 (789)
SR	14,234 (1,054)	13,475 (1,231)	14,186 (1,174)
SLM	7,992 (1,060)	7,493 (792)	8,547 (1,058)
	GAD67/CA3		
Total	46,000 (731)	24,459 (723)	27,819 (449)
SO	12,892 (1,302)	7,076 (639)	7,019 (747)
SP	13,800 (812)	6,613 (538)	8,064 (802)
SR	12,740 (751)	6,789 (626)	8,595 (1,082)
SLM	6,565 (731)	3,867 (449)	4,002 (723)
	GAD67/DG		
Total	33,993 (1,694)	23,512 (1,409)	19,027 (1,282)
GC	17,233 (1,429)	12,169 (990)	10,907 (1,159)
ML	11,351 (1,254)	6,172 (797)	5,337 (518)
Hilus	5,409 (318)	5,171 (193)	2,784 (195)
NeuN/hilus	24,781 (2,315)	24,027 (2,508)	24,684 (2,748)
NPY/hilus	5,073 (321)	4,895 (356)	5,073 (524)
SOM/hilus	5,616 (155)	5,427 (198)	3,276 (247)
SOM/CA3-SO	6,851 (519)	3,779 (117)	3,761 (201)

[1] Values represent the group mean with the standard error of the mean in parenthesis. GAD67, glutamic acid decarboxylase-67; SOM, somatostatin; NPY, neuropeptide Y; NeuN, neuronal nuclei protein; DG, dentate gyrus; SO, stratum oriens; SP, stratum pyramidal; SR, stratum radiatum; SLM, stratum lacunosum-moleculare; GC, granule cell layer; ML, molecular cell layer.